




Lignin activated carbon obtained by a environmentally friendly green production process using deep eutectic solvents

Deniz Aydemir,  Forest Industrial Engineering, Faculty of Forestry, Bartın University, Bartın, Turkey
Mehmet Emin Ergun,  Forestry and Forest Products, Akseki Vocational Schools, Alanya Alaaddin Keykubat University, Alanya, Turkey

Sezgin Koray Gulsoy,  **Zeynep Eda Ozan**,  Forest Industrial Engineering, Faculty of Forestry, Bartın University, Bartın, Turkey

Gokhan Gunduz,  Industrial Engineering, Faculty of Engineering and Natural Sciences, Iskenderun Technical University, Iskenderun, Turkey

Received August 11 2023; Revised November 24 2023; Accepted December 4 2023;
 View online 23 December, 2023 at Wiley Online Library (wileyonlinelibrary.com);
 DOI: 10.1002/bbb.2576; *Biofuels, Bioprod. Bioref.* 18:251–264 (2024)

Abstract: The aim of this study was to produce activated carbon (AC) from lignin obtained with deep eutectic solvents (DESs) of choline chloride–lactic acid. For this, lignin particles were produced using the DES. The DES lignin (DES-Lig) was modified with zinc dichloride, and the lignin activated carbon (lig-AC) was produced by carbonization at 600 and 900 °C. In this study, the AC obtained from the commercial lignin was also used to determine the changes in the lig-AC from the lignin obtained with the DES. The material properties were investigated using Brunauer–Emmett–Teller (BET) surface analysis, scanning electron microscopy (SEM) and thermogravimetric analysis (TGA), and the structural properties were investigated with X-ray diffractometry (XRD) of the lig-ACs. The commercial and DES-Lig exhibited different microscopic morphologies. The surface area of the samples generally ranged from 504 to 698 g/cm², and they included both micro- and mesopores according to SEM characterization. The XRD analysis showed that the ACs obtained have an amorphous structure, and thermogravimetric analysis of the ACs exhibited similar thermal behavior to that in the literature. The best morphological structure was found in the ACs prepared from lignin with the DES at 900 °C according to the results of SEM, TGA, XRD and BET analysis. The proximate analysis showed that the best ACs contain 1.5% moisture, 6.5% volatile matter, 5.5% ash content and 86.5% fixed carbon. According to the elemental analysis, the amounts of essential elements, including C, H, N and O were investigated, and the best activated carbon was determined to be the DES-Lig at 900 °C according to BET and the proximate fixed carbon results. © 2023 The Authors. *Biofuels, Bioproducts and Biorefining* published by Society of Industrial Chemistry and John Wiley & Sons Ltd.

Key words: activated carbon; lignin; deep eutectic solvents; eco-friendly production

Introduction

Green biomass-derived products have attracted high levels of interest from both academic and industrial areas. Therefore, lignocellulosic wastes, including cellulose, lignin and hemicellulose, have considerable advantages owing to their environmentally friendly, natural, non-toxic natures.^{1,2} In particular, lignin is among the most abundant bio-based polymers, after cellulose and it can be obtained in high amounts (20–25 wt% of raw material) as a value-added waste after cooking with intense acidic and alkali processes in the paper-making industry.^{3,4} The global lignin production is estimated to be around 100 million tons annually.⁵ The majority of lignin is either burned as a low-grade fuel or disposed of as waste, which poses environmental and economic challenges. Therefore, there is a growing interest in developing efficient and sustainable methods for lignin valorization, that is, converting lignin into useful products with higher added value. One of the potential applications of lignin is the production of activated carbon (AC), which is a porous carbonaceous material with a large specific surface area and high adsorption capacity.⁶ Activated carbon has a wide range of uses in various fields, such as water purification, gas separation, energy storage, catalysis and biomedical engineering. Activated carbon can be produced from various carbonaceous precursors, such as coal, wood, coconut shells and biomass wastes.⁷ Among these precursors, lignin has some advantages, such as its abundance, low cost, renewable nature and high carbon content. Therefore, lignin activated carbon (lig-AC) exhibit superior adsorption performance after carbonization and activation.⁸ Generally, lignin obtained from black liquors after the paper pulping process produces activated carbon.^{9,10} However, the extraction of lignin during the pulping process traditionally involves the use of petrochemical-based chemicals, such as sulfuric acid, sodium hydroxide, sodium sulfide, sulfur dioxide and chlorine, which raises concerns regarding its environmental impact.^{11,12} This approach is not considered environmentally friendly. There is a need to develop new pretreatment methods that can effectively solubilize and fractionate lignin from biomass while preserving its original structure and not harming the environment.

A promising approach for lignin extraction is the use of deep eutectic solvents (DESs), which are liquid mixtures of hydrogen-bond donors (HBDs) and hydrogen-bond acceptors (HBAs) at certain molar ratios. Deep eutectic solvents have several advantages over conventional solvents, such as low vapor pressure, high thermal stability, low toxicity, biodegradability, easy synthesis and tunable physicochemical

properties.¹³ Deep eutectic solvents are effective solvents for lignocellulosic biomass processing, especially for lignin valorization.^{14,15} They can dissolve lignin from biomass with high selectivity and yield and also enable lignin property tailoring by modifying the types and ratios of HBDs and HBAs. Moreover, DESs can act as reaction media for lignin functionalization and upgrading by facilitating various chemical reactions, such as hydrolysis, oxidation, reduction, esterification and etherification. Among various types of DESs, choline chloride (ChCl)-based DESs are widely used for lignin extraction because of their low cost, high availability, and good solubility. Choline chloride can form DESs with various HBDs, such as urea, glycerol, ethylene glycol, lactic acid (LA), malonic acid, oxalic acid, etc.^{13,16} The choice of HBD affects the solvation ability and chemical reactivity of DESs toward lignin. For example, the ChCl-urea DES has been reported to dissolve lignin from wheat straw with high yield (80%) and purity (90%).¹⁷ The ChCl-glycerol DES has been found to selectively extract lignin from poplar wood with a high yield (85%) and low molecular weight distribution ($M_w = 1.2$ kDa).¹⁸ The ChCl-LA DES has been shown to fractionate lignin from corn stover with high yield (87%) and purity (95%).¹⁹ The method has been defined as green because the chemicals used for obtaining lignin from wood are less harmful to the environment than other traditional chemicals (NaOH, Na₂S, etc.).

Lignin is found in black liquor and is extracted industrially in pulp production. To recover the cooking chemicals, the black liquor is burnt. Meanwhile, valuable lignin is being burned. Traditional processes (such as Kraft) are time consuming and inefficient for extracting lignin from black liquor. Lignin may be readily extracted from the black liquor using the DES process (by adding water to the black solution). In the extraction process, DES treatment generally is not applied as an extra step. Previous studies, such as Islam *et al.*,²⁰ Rodríguez Correa *et al.*²¹ and Lin *et al.*,²² showed that lignin has a large surface area after modification with the chemicals, and it is a good alternative for AC production. However, the lignin particles used in the studies were generally produced with petroleum-based chemicals. Unfortunately, this limits the use of bio-based materials of lignin, and the production of lig-AC may cause negative effects on the environment. Lignin makes up 15–35% of lignocellulosic biomass, and ~100 million tons of this biopolymer are isolated yearly as waste materials from the paper and bioethanol industry. Less than 2% of this enormous quantity is currently commercialized as low-value products, such as surfactants and adhesives, while the rest is mainly burned. The application of this underutilized biopolymer is attractive from both a sustainability and an

economic point of view.^{23,24} Deep eutectic solvent lignin has some superior properties compared with Kraft lignin. For example, the molecular weight of DES lignin is lower than that of Kraft lignin.²⁵ Lignin, which has a low molecular weight, shows superior antioxidant activity.^{26,27} Therefore, in this study, the lignin was produced with a green process using a DES. There are few studies on the activated carbon of lignin obtained with green chemicals in the literature, and this study was conducted on the lig-AC from the lignin obtained with green chemicals and the material [Brunauer–Emmett–Teller (BET), scanning electron microscopy (SEM) and thermogravimetric analysis (TGA)] and structural properties (X-ray diffractometry, XRD) of the lig-AC from the lignin obtained with green chemicals were investigated. Then the effects of the green chemicals on properties of the lignin activated carbon with the modification of zinc dichloride (ZnCl_2) at different carbonation temperatures (600 and 900 °C) were determined.

Materials and methods

Materials

The European black pine (*Pinus nigra* Arn.) used in this study was obtained from Türkiye's Black Sea Region's Bartın Province. A 10 cm thick wood disk was cut at breast height from a pine log. The log was debarked and subdivided into four disks (of 2.5 cm thickness). The disks were manually chiseled to a size of $2.5 \times 1.5 \times 0.5$ cm to produce chips for pulping. Choline chloride (CAS no. 67-48-1) and LA (CAS no. 79-33-4) were purchased from Sigma-Aldrich as DES components.

DES preparation

For 60 min on a heated plate at 80 °C, the ChCl-LA (molecular ratio 1:9) was homogeneously mixed until a transparent colorless liquid was produced. The DES was kept in a vacuum desiccator until use. Commercial lignin was used to compare the properties of the activated carbon obtained from the lignin with the DES. The commercial Kraft lignin was supplied from Canadian Lignin Inc. Zinc dichloride and hydrochloric acid (HCl) were used to activate and clean the activated carbon, respectively. All chemicals used in this study were bought with analytic purity from Sigma-Aldrich (Darmstadt, Germany).

Lignin preparation with DES

The European black pine DES pulp was generated in a laboratory-sized 15 L rotary digester heated by electricity. A

700 g sample of oven-dried pine chips was used in the DES cooking. The DES cooking time and temperature were set at 4 h and 160 °C, respectively. In the DES pulping, the chip/DES solution ratio was 1:5. In the cooking process, 700 g of wood and 3500 g of DES solution were utilized. In other words, 5 g of DES solution was used for every 1 g of wood. The DES black liquor was extracted from the pulp after DES pulping by filtering. Distilled water (1:1 v/v) was added to the DES black liquor for lignin precipitation. Filter paper (Whatman no. 42) was used to filter the precipitated lignin. The obtained DES-lignin (DES-Lig) was oven dried for 24 h at 30 °C. A Willey mill was used to grind the dried samples. The holocellulose²⁸ and Klason lignin²⁹ contents of DES-Lig were determined as 32.4 and 67.0%, respectively. Water is an anti-solvent for the DES and was used as an anti-solvent for the precipitation of lignin. The hydrogen bond interaction between DES and lignin probably contributes to the lignin solubility in DES and subsequent extraction. This hypothesis is supported by the fact that after adding water to the DES–lignin mixture, lignin can easily separate from the DES.¹⁹ The humidity of DES-Lig samples dried in an oven at 30 °C for 24 h was measured as 6%. The pH value of 1:9 ChCl-LA was 1–2.

Production of activated carbon from lignin

The lignin produced from wood with a DES and commercial lignin was used at 50 g per formulation. A 50 g sample of lignin powder was added to a solution of 25 g ZnCl_2 (50% wt lignin) and 75 mL of distilled water. The lignin– ZnCl_2 /distiller water blends were maintained to complete the activation of the lignin at 20 ± 5 °C for 24 h, and they were dried at 80 °C for 24 h. The production of the activated carbon was conducted at 600 and 900 °C in a tube furnace (Henan Sante Furnace Technology Co. Ltd, model STG-40-14, Henan, China) under an argon gas flow of 60 mL/min. The obtained activated carbon was cooled at room temperature and later the activated carbon was rinsed with 0.5 M HCl until their pH value was at 6–6.5. After cleaning, the activated carbon was dried at 100 °C for 6 h, and later they were ground as given in Fig. 1. The yield values of activated carbon types obtained from lignin are shown in Table 1.

Methods

BET analysis

The activated carbon was cleaned by heating at 150 °C for 2 h in a vacuum before the isotherm was measured. Using the N adsorption isotherm, the BET technique was used to determine the activated carbon's surface area. The BET surface area and micropore volume of the activated carbon

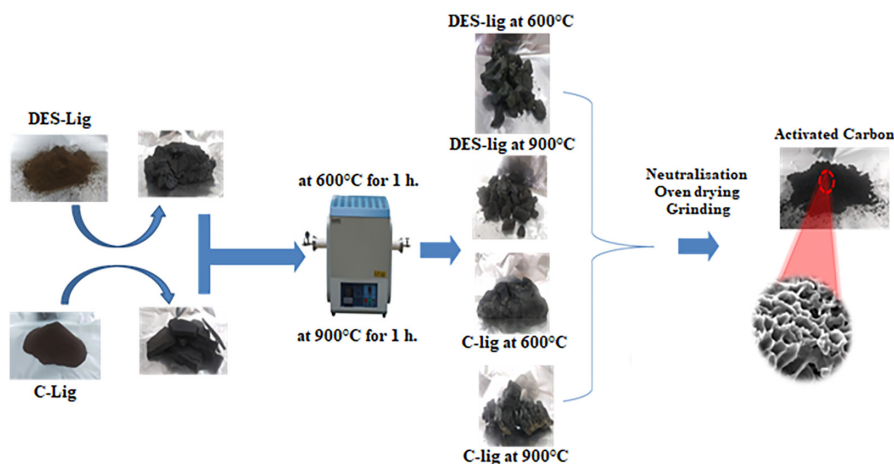


Figure 1. Production parameters of activated carbon types obtained from lignin.

Table 1. Yield values of activated carbon types obtained from lignin.

Samples	Sample codes	Yield (%)
Lignin obtained with deep eutectic solvents at 600 °C	DES-Lig at 600 °C	52.5
Lignin obtained with deep eutectic solvents at 900 °C	DES-Lig at 900 °C	33.8
Commercial lignin at 600 °C	C-Lig at 600 °C	68.9
Commercial lignin at 900 °C	C-Lig at 900 °C	47.3

Abbreviations: DES, deep eutectic solvent; DES-Lig, DES lignin.

were determined using N_2 adsorption/desorption isotherm tests conducted on a Quantachrome autosorb IQ model BET instrument. The micropore volume was determined using the Dubinin–Radushkevich equation. The macro pore volume was determined using the Gurvich rule at $P/P_0 = 0.95$. P : The partial pressure of adsorbate gas in equilibrium with surface, in pascals, P_0 : The saturated pressure of adsorbate gas, in pascals. The mesopore volume was calculated as the difference between the total pore volume and the micropore volume according to the IUPAC report.³⁰

Morphological analysis

The morphological structures of the obtained activated carbon was examined using scanning electron microscopy (Tescan MAIA3 XMU-SEM) at the same magnitudes. They were coated to increase the electron conductivity with gold/palladium using a Denton spray coater.

XRD analysis

X-Ray diffraction was conducted with a Philips PANalytical Empyrean X-ray diffractometer using Ni-filtered $Cu K\alpha$ (1.540562 \AA) radiation. The obtained activated carbon was scanned from 10° to $80^\circ 2\theta$ range and the crystallinity of the samples was calculated using the Segal and curve fitting methods as given in the formulation:

$$\text{CrI} (\%) = \frac{\Sigma A_c}{\Sigma (A_a + A_c)} \times 100$$

where A_c is the integrated area underneath the respective crystalline peaks and A_a is the integrated area of the amorphous halo.

TGA

Thermal analysis was conducted on a sample amount of 5 mg with a Perkin Elmer tester. The test was performed from 25 to 1200 °C at a 20 °C/min heating rate under a nitrogen flow at 20 mL/min to prevent oxidation. The TGA curves were used to calculate the temperatures at which the activated carbon lost 10 and 50% of its mass ($T_{10\%}$ and $T_{50\%}$), as well as the temperature at which it decomposed at the highest rate (DTGmax).

Proximate and ultimate analysis

Proximate analysis was conducted on a 2–3 mg sample with a Perkin Elmer tester. The analysis parameters are given in Fig. 2.

According to the TGA method for proximate analysis, the moisture (M), volatile matter (VM), ash (A) and fixed carbon (FC) were calculated according to the parameters in Fig. 2:

$$M = \frac{W - B}{W}$$

$$VM = \frac{B - C}{W}$$

$$A = \frac{D}{W}$$

$$FC = 1 - (M + A + VM)$$

The ultimate analysis was on a 1–2 mg sample with a Eurovector EA3000-Single. The elemental analyzer is a device that determines the carbon, hydrogen and nitrogen elements in percentages by chromatographic methods by burning a solid or liquid organic compound weighed in milligrams at a high temperature of approximately 1000 °C with high-purity oxygen gas.

Results and discussion

Proximate and ultimate analysis

The proximate and ultimate analyses were conducted to determine some parameters, including the amount of moisture, ash, volatile matter, fixed carbon, and elemental composition of the activated carbon. The moisture represents the amount of water in the samples as a percentage of the weight. Ash is the amount of residue left after the samples are completely burned. The volatile matter in the samples

comprises the condensable vapor and the gases (except for water vapor) released from biomass when heated. Fixed carbon is the solid combustible residue that remains after the condensable vapor, the gases, and the volatile matter are removed.³¹

The TGA analysis provided the proximate data for the weight changes in the materials according to the related process in the Materials and methods. The proximate results are given in Fig. 3 and Table 2. The TGA showed that the samples before the carbonization process [C-Lig (commercial lignin) and DES-Lig] exhibited a different thermal behavior than the others, and C-Lig and DES-Lig had a higher degradation at 15–30 min, while the activated carbon and C-Lig and DES-Lig showed more mass loss. As seen in Table 2, the moisture of samples was determined to change in the range of 1.5–6.4%, and the volatile contents generally were high (57.8% and 66.9%) for the C-Lig and DES-Lig; however, the value for the activated carbon ranged from 6.5 to 23.4%. The ash content ranged from 1.5 to 6.2%, and while the fixed carbon values for the DES-Lig and C-Lig samples were 23.5 and 35.5, respectively, those for the other samples were calculated to change in a range of 70–86.5%. As seen in Table 2, the temperature affects both the volatile matter and the fixed carbon of the ACs obtained from both materials and while the temperature was raised from 600 to 900 °C, the volatile matter decreased; the fixed carbon amount was found to increase. Mendez *et al.*³⁶ conducted a proximate analysis of sub-bituminous coals, and the moisture and ash contents were in the ranges 0.7–2.9 wt% and 0.2–2.2 wt%, respectively.

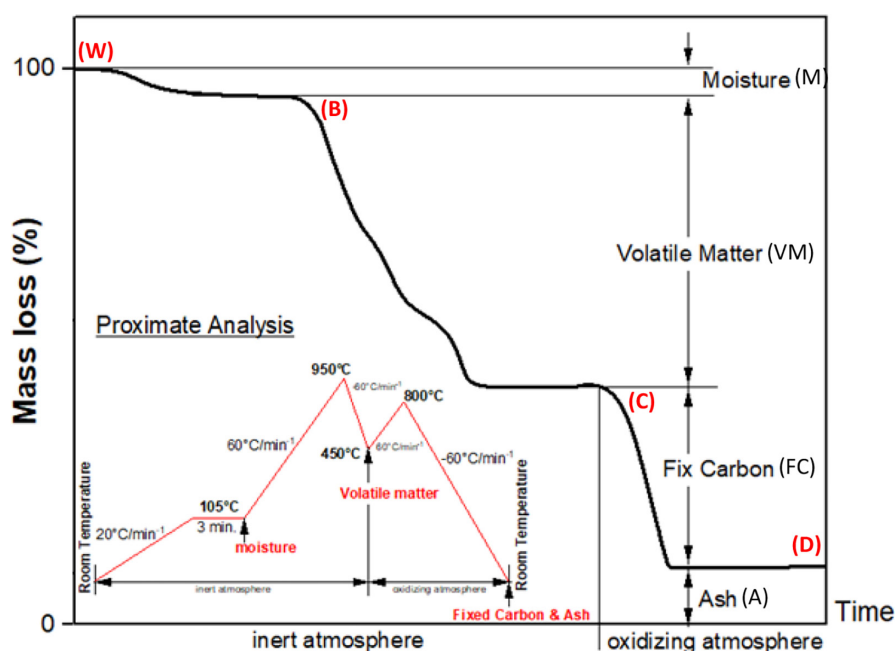


Figure 2. Analysis parameters during proximate thermogravimetric analysis (TGA).^{31–35}

The fixed carbon and the volatile matter were calculated in the ranges 39.8–50.8 and 48.1–58.1 wt%, respectively. The proximate analysis results for the activated carbon from biomass were calculated as 3–5% for moisture, 1–3% for ash, 11–42% for volatile matter and 50–85% for fixed carbon in the previous studies.^{31,37–40} The results of this study are agreement with the previous results. The parameters, including moisture, ash and volatile matter, help to examine the residual carbon amount in the activated carbon, and a high fixed carbon content is desirable for activated carbon. In this study, the highest fixed carbon was determined at a percentage of >80% in the activated carbon prepared at 900 °C. The best activated carbon was determined to be the DES-Lig at 900 °C according to the BET and proximate fixed carbon results.

The elemental compositions of C-Lig and DES-Lig (samples before carbonization) using ultimate analysis (Table 2) showed the existence of carbon at 32.1 and 38.8%, oxygen at 56 and 62.8%, nitrogen at 0.1 and 0.5% and hydrogen at 4.7

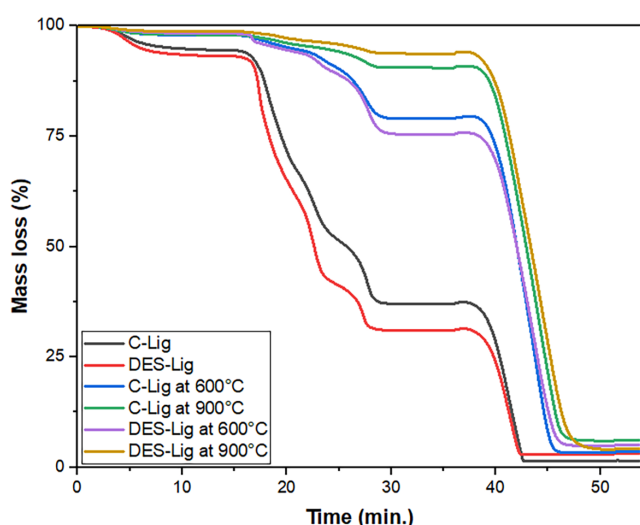


Figure 3. Proximate analysis curves of all activated carbon and the materials before carbonization.

and 5%, respectively. For activated carbon, carbon, oxygen, nitrogen and hydrogen were found in the ranges 63.5–83.6%, 15.2–33.9%, 0.2–0.8% and 1–2.4%, respectively. The ACs obtained at a high temperature of 900 °C had a low content of O owing to removal of the oxygen groups containing functional groups.^{31,40}

BET analysis

The BET adsorption/desorption isotherm graphs of activated carbon produced from DES-Lig and C-Lig using $ZnCl_2$ as an activating agent are given in Fig. 4.

The N_2 adsorption/desorption isotherms of the produced activated carbon samples were examined. The nitrogen adsorption/desorption isotherms of the activated carbon samples reveal characteristics that can be associated with both microporous and mesoporous materials. They exhibit an increasing adsorbed volume at low relative pressures, resembling a Type I isotherm indicative of microporous materials with pore sizes smaller than 20 Å. However, they also show a slowly expanding hysteresis loop at intermediate relative pressures, resembling a Type IV isotherm associated with nitrogen capillary condensation in mesoporous structures with pore sizes ranging from 20 to 500 Å.^{41,42} This combination suggests the presence of both micropores and mesopores in the activated carbon. The hysteresis loop observed in the isotherm indicates the development of mesopores during the activation/carbonization process, as supported by previous studies.⁴³ Furthermore, the micropore volume and fraction are found to be higher than the mesopore volume and fraction in all samples, which is consistent with the pore size distribution data provided in Table 3. Both micropores and mesopores exhibited an increase as the treatment temperature rose, so, activated carbon which produced at 900 °C has a higher porosity than activated carbon which produced at 600 °C. Similar to the result, Huang *et al.*⁴⁴ found that the activation temperature has a significantly positive effect on the micro-

Table 2. Proximate and ultimate analysis curves of all activated carbon and the materials before the carbonization.

Samples	Elemental analysis (%)				Proximate analysis (%)			
	C	H	N	O	Moisture	Volatile	Ash	Fixed carbon
C-Lig	38.8	4.7	0.5	56	5.2	57.8	1.5	35.5
DES-Lig	32.1	5.0	0.1	62.8	6.4	66.9	3.2	23.5
C-Lig at 600 °C	65.9	2.3	0.8	31	2.1	19.4	3.5	75
C-Lig at 900 °C	74.0	1.9	0.7	23.4	2.0	7.7	6.2	84.1
DES-Lig at 600 °C	63.5	2.4	0.2	33.9	1.7	23.4	4.9	70.0
DES-Lig at 900 °C	83.6	1.0	0.2	15.2	1.5	6.5	5.5	86.5

Abbreviations: DES, deep eutectic solvent; DES-Lig, DES lignin.

and mesoporosity. The BET analysis results of the produced activated carbon samples are given in Table 3.

The yield of activated carbon decreased with an increase in temperature for both types of lignin. For lignin obtained with deep eutectic solvents, the yield decreased from 52.5% at 600 °C to 33.8% at 900 °C. Similarly, for commercial lignin, the yield decreased from 68.9% at 600 °C to 47.3% at 900 °C. As the temperature increases, the reason behind the decrease in the yield of activated carbon in the DES-Lig and C-Lig samples is the increased thermal degradation and volatilization of the carbonaceous material. This situation led to a reduction of the mass of material. Simultaneously, the temperature increased for both samples, and the surface area and total pore volume of activated carbon increased. Higher temperatures accelerate the activation process, forming more pores on the surface and within the structure of the carbon material. The micropore volume of activated carbon increased with temperature for both samples. Therefore, high temperatures supported the formation of micropores, which were more stable and resistant to collapse.⁴⁵ The mesopore volume of activated carbon also increased with rising temperature, but to a lesser extent than the micropore

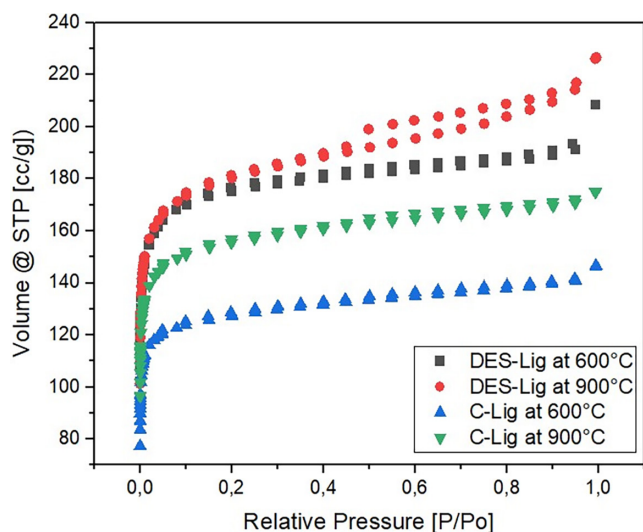


Figure 4. Nitrogen gas adsorption/desorption isotherm of activated carbon produced from deep eutectic solvent (DES) lignin (DES-Lig) and C-Lig.

volume. The high temperatures can lead to some mesopores forming; however, these mesopores are more prone to merging and closing. The average pore diameter remained almost constant with increasing temperature for DES-Lig samples but increased slightly for C-Lig samples. This difference is attributed to the fact that both micropore and mesopore volumes influence the average pore diameter, and these changes depend on the type and source of lignin. In general, carbonization temperatures exceeding 600 °C lead to an increase in the rates of liquid and gas release while causing a decrease in activated carbon yield.^{46,47} Higher temperatures also contribute to an increase in ash and fixed carbon content while reducing the quantity of volatile matter. Therefore, elevated temperatures result in higher-quality activated carbon but simultaneously lead to a decrease in yield.⁴⁷⁻⁴⁹

The properties of activated carbon obtained from DES-Lig and C-Lig using $ZnCl_2$ as activating agents were investigated. Nitrogen adsorption–desorption isotherms were used to determine the pore diameter, surface area and pore volume of the activated carbon. The results indicated that DES-Lig-600 and DES-Lig-900 had higher pore volume and surface area than C-Lig-600 and C-Lig-900, respectively. $ZnCl_2$ is commonly used as an activator in the production of activated carbon from biomass. It facilitates the removal of hydrogen and oxygen from the biomass structure in the form of water, thereby exerting a favorable activation effect.⁵⁰ $ZnCl_2$ does not react with carbon and can eliminate hydrogen and oxygen atoms from the activated carbon structure.⁵¹ When $ZnCl_2$ is utilized as an activating agent, it inhibits the formation of tar and other impurities that could obstruct the activated carbon surface and impede the passage of volatile compounds. As a result, the yield is higher than that for carbon activated with potassium hydroxide.⁵² This enhancement of condensed aromatic reactions and its influence on polymerization reactions lead to the exclusion of certain active sites from neighboring molecules.⁵³

The cellulose in DES-Lig swelled during $ZnCl_2$ activation owing to the electrolytic impact on its molecular structure.⁵⁴ This swelling increased the surface area of the activated carbon by fragmenting cellulose molecules and increasing internal and interlayer gaps.⁵⁵⁻⁵⁷ The conversion of lignocellulosic raw materials into activated carbon is

Table 3. BET analysis results of activated carbon produced from DES-Lig and C-Lig.

Samples	Surface area (m ² /g)	V _{micro} (cm ³ /g)	V _{meso} (cm ³ /g)	V _{total} (cm ³ /g)	D _p (Å)
DES-Lig at 600 °C	688	0.240	0.059	0.299	19.14
DES-Lig at 900 °C	698	0.244	0.092	0.336	19.08
C-Lig at 600 °C	504	0.180	0.039	0.219	15.28
C-Lig at 900 °C	610	0.216	0.050	0.266	19.13

Abbreviations: BET, Brunauer–Emmett–Teller; DES, deep eutectic solvent; DES-Lig, DES lignin.

accompanied by the release of oxygen, hydrogen atoms, carbon dioxide, carbon monoxide, aldehydes and methane, which leads to the formation of pyrolysis distillates.⁵⁸ Consequently, DES-Lig exhibits a higher surface area compared with C-Lig. Furthermore, it was observed that the surface area increases with higher temperatures. However, carbonization temperatures above 600 °C can decrease the yield of activated carbon and increase the rate of liquid and gas release. High temperatures also increase the ash and fixed carbon content while reducing the amount of volatile matter.^{49,59} Thus, high temperatures enable the production of activated carbon with a higher surface area but at the expense of reduced yield.⁴⁸ Consequently, the activated carbon produced in this study exhibited specific surface areas ranging from 504 to 698 m²/g, micropore volumes between 0.180 and 0.244 cm³/g and mesopore volumes between 0.039 and 0.092 cm³/g, as presented in Table 3. Studies were conducted on producing activated carbon using lignin obtained from black liquors. Various chemical activators,

such as KOH¹⁰, HCl, HNO₃ and H₃PO₄ were utilized, along with temperatures ranging from 500 to 900 °C.⁶⁰ The surface area of the produced lignin-based activated carbon was found to be between 86 and 1509 m²/g.^{9,61} The results within the scope of the present study were found to be similar.

Morphological characterization

The SEM images and morphological structure of the activated carbon obtained from DES-Lig and C-Lig at 600 and 900 °C are shown in Figs 5 and 6, respectively.

The SEM analyses examined the morphology of the activated carbon. The SEM image at 20 μm for both 600 and 900 °C (Fig. 5) showed that the surfaces of the activated carbon are smooth and flat, and the SEM images at the magnitudes of 1 μm and 500 nm showed that the activated carbon had a porous structure. The morphological structures of the activated carbon obtained from C-Lig at 600 and 900 °C were found to exhibit similar morphologies. The

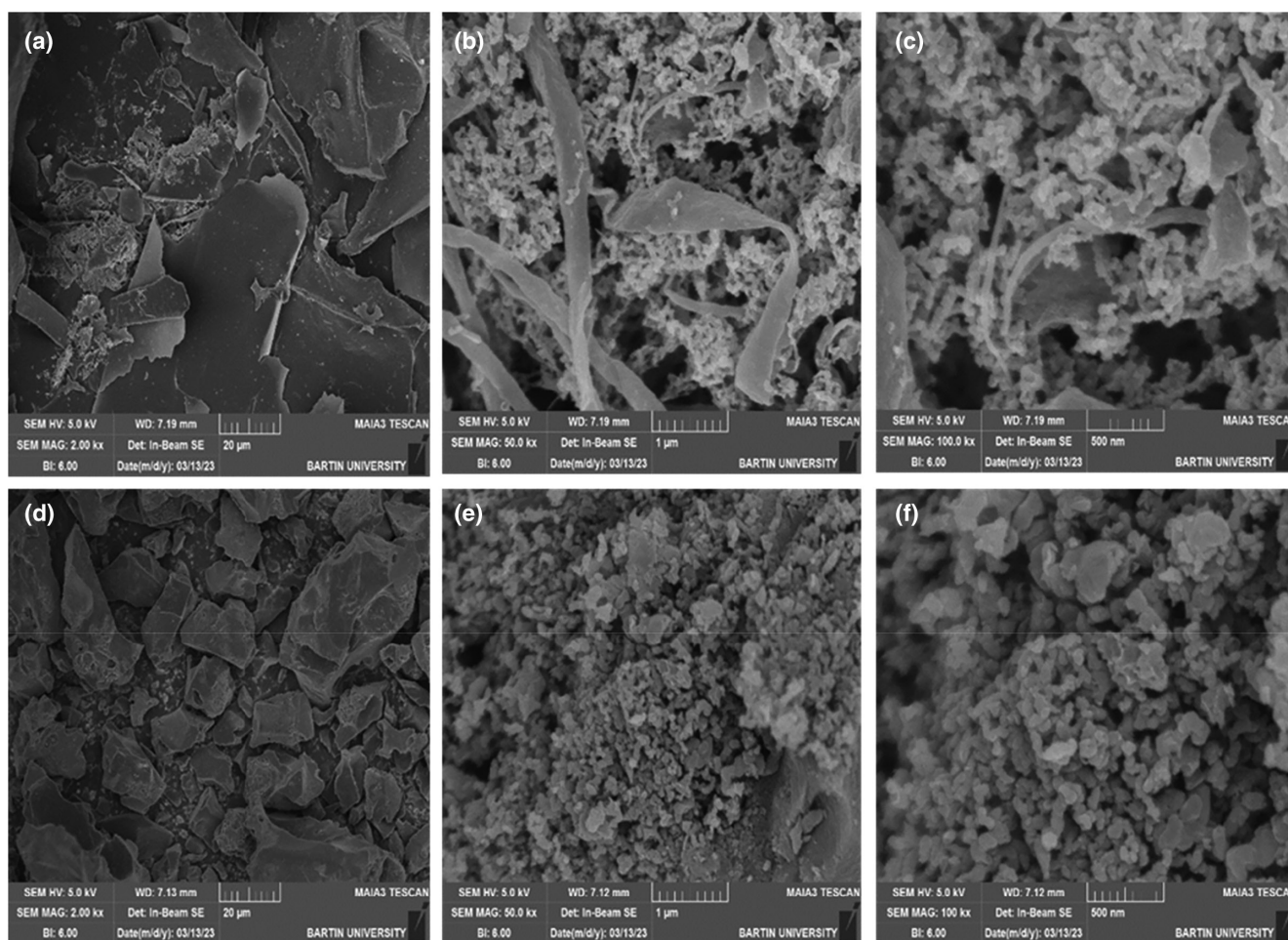


Figure 5. Scanning electron microscopy (SEM) images of the activated carbon prepared at 600 and 900 °C from lignin obtained with DES.

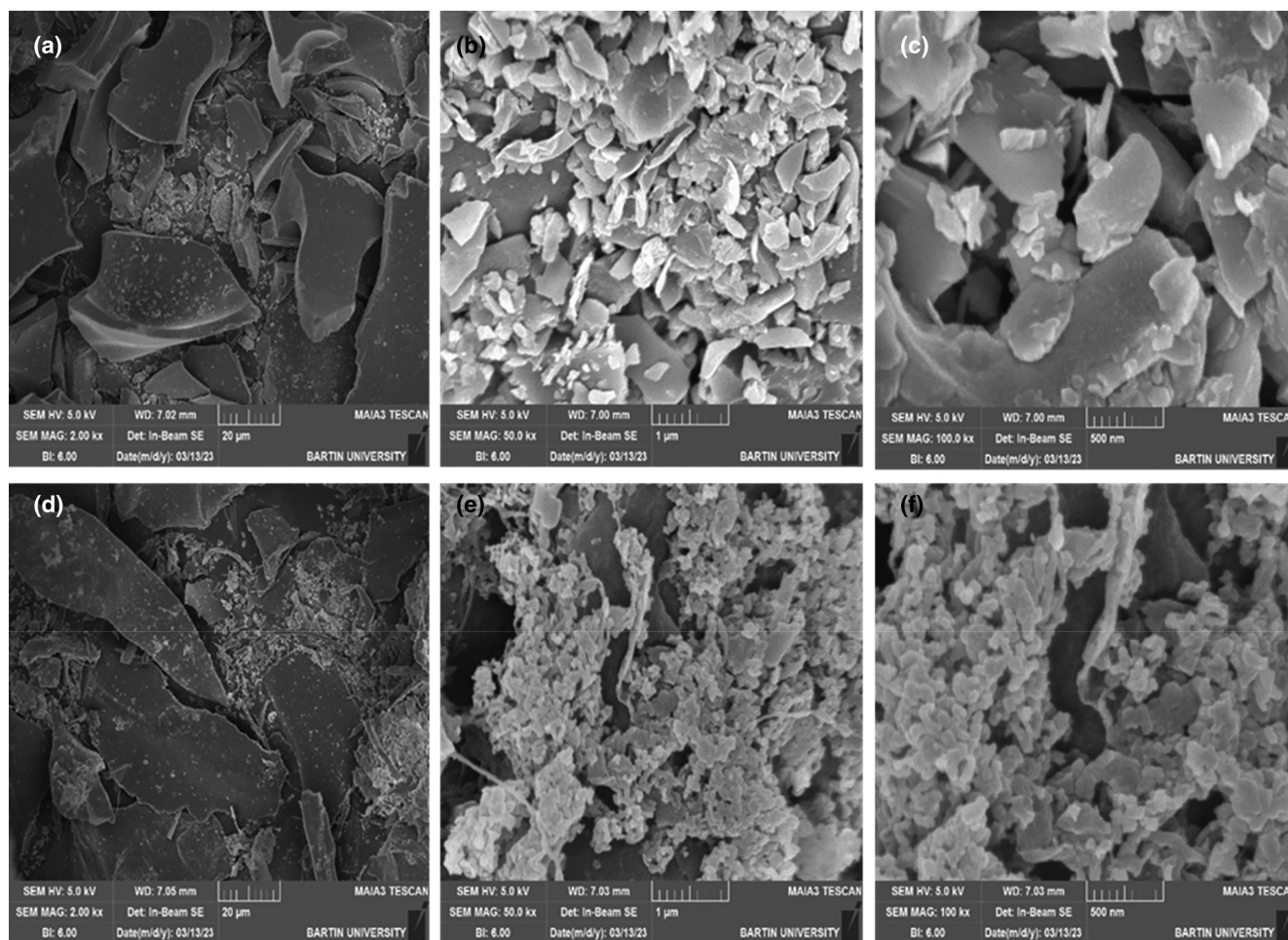


Figure 6. SEM images of the activated carbon prepared at 600 and 900 °C from commercial lignin.

activated carbon prepared at 600 °C were found to have some impurities, including carbonized cellulosic fibers, whereas the activated carbon prepared at 900 °C was found to not have any impurities, and the activated carbon was determined to have smaller particles and lower porosities. Figure 5 shows SEM images of the activated carbons obtained from DES-Lig at 600 and 900 °C.

According to the SEM image at 20 μm for both 600 and 900 °C (Fig. 6), the activated carbon had smooth and flat surfaces, and the SEM images at the magnitudes of 1 μm and 500 nm showed that the activated carbon had a nano-porous structure. The morphological structures of the activated carbon obtained from DES-Lig at 600 and 900 °C were found to exhibit similar morphologies, and when the temperature rose from 600 to 900 °C, the diameter of the activated carbon was found to get smaller. The activated carbon prepared at both 600 and 900 °C generally exhibited a rigid structure, as presented in De Rose *et al.*⁶² and Cai *et al.*³¹ As a result, the activated carbon prepared at both 600 and 900 °C had a rigid activated carbon structure. However, the DES and CL

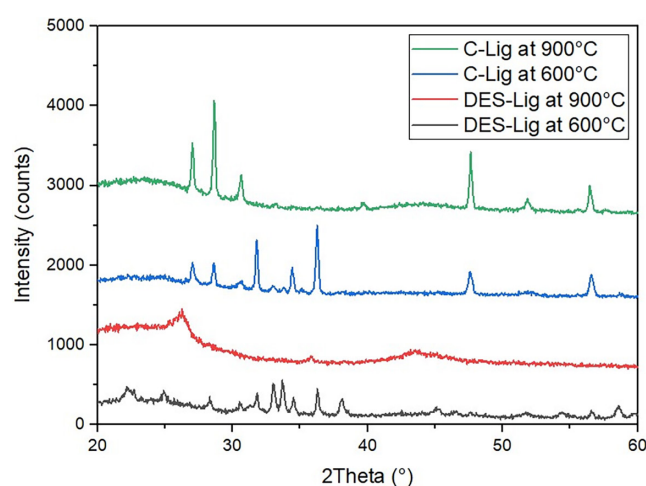


Figure 7. X-Ray diffraction (XRD) spectra of the activated carbon obtained from DES-Lig and C-Lig.

activated carbon prepared at 900 °C consisted of smaller and more similar sized particles as shown in Figs 5 and 6, but the SEM morphology of the activated carbon prepared from both

Table 4. Summary results of X-ray diffraction spectra of the activated carbon.

Samples	2 θ (deg)	Crystallinity (%)
DES-Lig at 600 °C	22, 25, 27, 32, 33, 33.8, 34.5, 36, 38, 58.6	35
DES-Lig at 900 °C	26.5, 44	22
C-Lig at 600 °C	27, 28.6, 31.8, 34.5, 36.2, 46.5, 56.5	38
C-Lig at 900 °C	27, 28.6, 30.6, 47.6, 51.8, 56.5	30

Abbreviation: DES, deep eutectic solvent; DES-Lig, DES lignin.

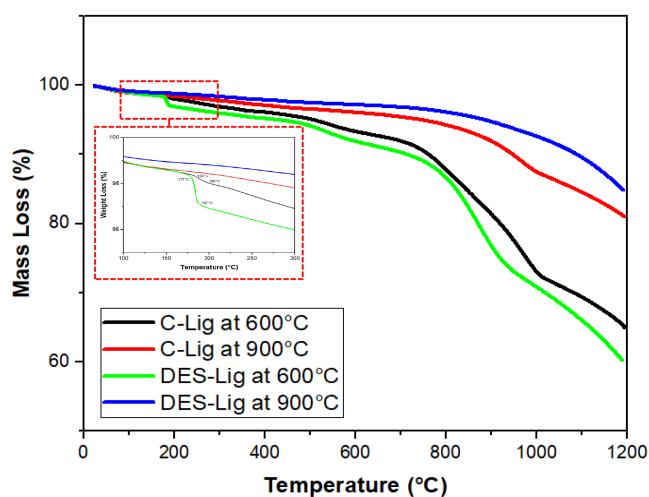


Figure 8. TGA of the activated carbon.

DES-Lig and C-Lig at 600 and 900 °C showed that the particle size and pore size generally were below 1 μm . The activated carbon surfaces were found generally to be smooth and flat in many studies and this shows that the activated carbon was successfully produced.^{10,63-66} This study's results showed that lignin will be a good choice for activated carbon production and the results of the studies conducted by Demirbas,⁶⁷ and Allen *et al.*⁶⁸ agree with our results.

XRD analysis

X-ray diffraction is a basic method for determining the carbon stacking structure of the activated carbon. Therefore, the changes in the structural properties of the activated carbon caused by the carbonization temperatures and production type of lignin were examined with XRD, as given in in Fig. 7.

Lignin has an amorphous structure, and it generally exhibits a peak at about 21–23° depending on the production type.² After treatment with ZnCl_2 and activating at high temperatures, lignin-activated carbon exhibited several peaks

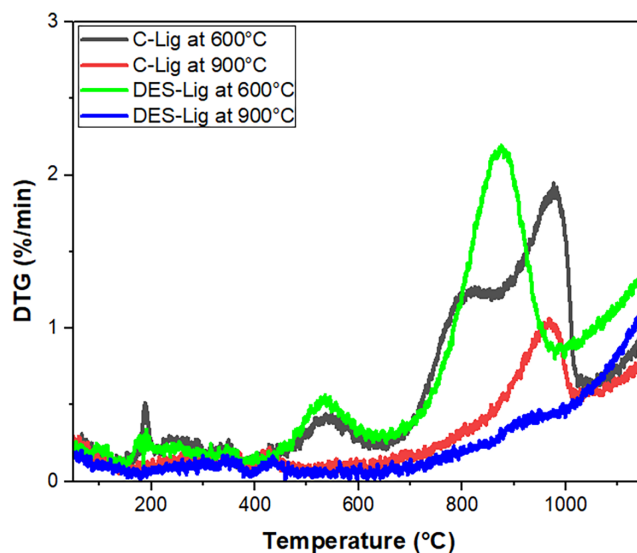


Figure 9. DTG analysis of the activated carbon.

Table 5. Summary results of TGA and DTG curves of the activated carbon.

Samples	T10% (°C)	T50% (°C)	DTGmax (°C)	Mass loss (%)
DES-Lig at 600 °C	710	–	976	35
DES-Lig at 900 °C	1080	–	970	29
C-Lig at 600 °C	760	–	875	40
C-Lig at 900 °C	943	–	1150	16

Abbreviations: DES, deep eutectic solvent; DES-Lig, DES lignin; DTGmax, temperature with decomposition at the highest rate; TGA, thermogravimetric analysis.

at 25–27°, 37–40° and 48–50° owing to the presence of ZnCl_2 . However, the activated carbon of DES-Lig at 900 °C showed a different behavior than the others and its peaks were at 26°, 35° and 46° owing to the possible presence of ZnCl_2 . The lignin activated carbon generally has two peaks at about 26.0 and 44.0° corresponding to graphite.^{69,70} Table 4 shows the summary results of the XRD spectra of the activated carbon.

With the help of Origin software, the crystallinity of the samples was calculated. The highest crystallinity was found to be 35% for DES-Lig at 600 °C and the lowest crystallinity was determined as 22% for DES-Lig at 900 °C owing to the increasing porosity of the activated carbon with raised activation temperatures. As seen in the SEM images in Figs 5 and 6, the increase in porosity can be seen with a rise in treatment temperature and the porosity increase the amorphous structure.⁶² As a result, DES-Lig exhibited a higher amorphous structure than C-Lig according to the XRD pattern. Additionally, the crystallinity index results showed that DES-Lig at 900 °C had higher amorphous structure than the other

samples. Many previous studies have shown that activated carbon has a higher surface area when the amorphous structure increases.^{37,45,51} The BET results show that the highest surface area was obtained in DES-Lig at 900°C, and it can be said that the results were supported by the BET and SEM results.

TGA

Thermogravimetric analysis of the activated carbon was conducted from room temperature to 1200°C. The thermogravimetric (TGA) and derivative thermogravimetric (DTG) curves are presented in Figs 8 and 9.

The TGA curves showed the degradation behavior of the activated carbon and thermal decomposition temperatures (T_{onset}) occurred at 170–185°C. The T_{onset} was found at 177°C for DES-Lig produced at 600°C and the T_{onset} was determined to be 183°C for C-Lig prepared at 600°C. This was caused by the low purity of the activated carbon prepared at 600°C. The DTGmax was determined using the DTG curves, and the DTGmax of the activated carbon generally was found to be above 800°C as seen in Fig. 9.

Table 5 shows a summary of TG analysis of the activated carbon and all samples generally exhibit at $T_{10\%}$ and no samples did not indicate a degradation of $T_{50\%}$ due to exhibiting large mass loss at high temperatures (above 1200°C). Mass loss occurred at 16–35%. The lowest and highest mass loss was calculated as 16% for the C-Lig prepared at 900°C and 35% for the DES-Lig prepared at 600°C, respectively. The DTGmax ranged from 875 to 976°C.

The results of this study are consistent with those reported by Dittmann *et al.*,⁷¹ who found that activated carbon prepared by chemical activation with zinc chloride had higher thermal stability than those prepared by physical activation. However, they are different from those reported by Kaya *et al.*⁷² who found that activated carbon prepared from pistachio shells by chemical activation with zinc chloride had lower thermal stability than those prepared by physical activation.

Conclusion

Activated carbon with commercial Kraft lignin and lignin prepared with green solvents (DESs) as a carbon source were successfully prepared at different activation temperatures by a carbonization-activation method using ZnCl_2 . The commercial lignin and DES-Lig exhibit different microscopic morphologies, and the surface areas of the samples generally range from 504 to 698 g/cm^2 and include both micro- and mesopores. The best morphological structure was found in the activated carbon prepared from lignin with a DES at 900°C according to the results of SEM, TGA, XRD and

BET analysis. It can be said that the lignin prepared with DES delignification can be a good alternative as a bio-based material source for activated carbon production.

Author contributions

I declare that all the authors had significant participation in the development of this work. Deniz Aydemir helped with all tests and prepared the original draft, Mehmet Emin Ergun produced the activated carbon and wrote and edited the original draft, Sezgin Koray Gulsoy prepared the lignin with deep eutectic solvents and edited the original draft, Zeynep Eda Ozan helped all tests and edited the original draft, and Gokhan Gunduz helped in all tests and edited the original draft.

Acknowledgements

We would like to express our sincere gratitude to TÜBİTAK ULAKBİM for covering the open access publication fees associated with this work.

Conflict of interest

The authors declare that they have no known conflict of interest or personal relationships.

References

1. Yang Z, Gleisner R, Mann DH, Xu J, Jiang J and Zhu JY, Lignin based activated carbon using H_3PO_4 activation. *Polymers* **12**:2829 (2020).
2. Gencer A, Akyüz M, Yurdakurban F and Aydemir D, Characterization and separation of lignin from kraft black liquor with different alcohols. *Drv Ind* **73**:405–413 (2022).
3. Anuchi SO, Campbell KLS and Hallett JP, Effective pretreatment of lignin-rich coconut wastes using a low-cost ionic liquid. *Sci Rep* **12**:6108 (2022).
4. Elkholy AS, Yahia MS, Elnwawy MA, Gomaa HA and Elzeref AS, Synthesis of activated carbon composited with Egyptian black sand for enhanced adsorption performance toward methylene blue dye. *Sci Rep* **13**:4209 (2023).
5. Bajwa DS, Pourhashem G, Ullah AH and Bajwa SG, A concise review of current lignin production, applications, products and their environmental impact. *Ind Crops Prod* **139**:111526 (2019).
6. Koyuncu F, Avşar Teymur Y and Güzel F, Application of an industrial agricultural waste-based activated carbon in the treatment of water contaminated with reactive blue 19 dye: Optimization, kinetic, equilibrium and recyclability analyses. *J Dispers Sci Technol* **44**:2565–2576 (2023).
7. Güzel F and Koyuncu F, Conversion of citrus industrial processing solid residues to well-developed mesoporous powder-activated carbon and its some water pollutant removal performance. *Biomass Convers Biorefin* **13**:2363–2374 (2023).

8. Supanchaiyamat N, Jetsrisuparb K, Knijnenburg JT, Tsang DCW and Hunt AJ, Lignin materials for adsorption: Current trend, perspectives and opportunities. *Bioresour Technol* **272**:570–581 (2019).
9. Fu K, Yue Q, Gao B, Sun Y and Zhu L, Preparation, characterization and application of lignin-based activated carbon from black liquor lignin by steam activation. *Chem Eng J* **228**:1074–1082 (2013).
10. Khezami L, Chetouani A, Taouk B and Capart R, Production and characterization of activated carbon from wood components in powder: Cellulose, lignin, xylan. *Powder Technol* **157**:48–56 (2005).
11. Fang Z and Smith RL Jr, *Production of Biofuels and Chemicals from Lignin*. Springer, Singapore, pp. 379–418 (2016).
12. Kihlman J and Gustavsson C, The feasibility of utilizing existing process streams in Kraft pulp mills as a source of chemicals for lignin extraction. *BioResources* **16**:1009–1028 (2021).
13. Alonso DM, Wettstein SG and Dumesic JA, Bimetallic catalysts for upgrading of biomass to fuels and chemicals. *Chem Soc Rev* **41**:8075–8098 (2016).
14. Chen Z, Ragauskas A and Wan C, Lignin extraction and upgrading using deep eutectic solvents. *Ind Crops Prod* **147**:112241 (2020).
15. Hong S, Shen XJ, Xue Z, Sun Z and Yuan TQ, Structure–function relationships of deep eutectic solvents for lignin extraction and chemical transformation. *Green Chem* **22**:7159–7180 (2020).
16. Wagle DV, Zhao H and Baker GA, Deep eutectic solvents: Sustainable media for nanoscale and functional materials. *Acc Chem Res* **47**:2299–2308 (2014).
17. Ma H, Fu P, Zhao J, Lin X, Wu W, Yu Z *et al.*, Pretreatment of wheat straw lignocelluloses by deep eutectic solvent for lignin extraction. *Molecules* **27**:7955 (2022).
18. Alvarez-Vasco C, Ma R, Quintero M, Guo M, Geleynse S, Ramasamy KK *et al.*, Unique low-molecular-weight lignin with high purity extracted from wood by deep eutectic solvents (DES): A source of lignin for valorization. *Green Chem* **18**:5133–5141 (2016).
19. Lou R, Ma R, Lin KT, Ahamed A and Zhang X, Facile extraction of wheat straw by deep eutectic solvent (DES) to produce lignin nanoparticles. *ACS Sustain Chem Eng* **7**:10248–10256 (2019).
20. Islam MS, Ang BC, Gharekhani S and Afifi ABM, Adsorption capability of activated carbon synthesized from coconut shell. *Carbon Lett* **20**:1–9 (2016).
21. Rodríguez Correa C, Stolovsky M, Hehr T, Rauscher Y, Rolli B and Kruse A, Influence of the carbonization process on activated carbon properties from lignin and lignin-rich biomasses. *ACS Sustain Chem Eng* **5**:8222–8233 (2017).
22. Lin J, Xue F and Zhao G, Soda lignin-based activated carbon and its adsorption properties. *BioResources* **14**:376–386 (2019).
23. Boarino A and Klok HA, Opportunities and challenges for lignin valorization in food packaging, antimicrobial, and agricultural applications. *Biomacromolecules* **24**:1065–1077 (2023).
24. Shishov A, Bulatov A, Locatelli M, Carradori S and Andruch V, Application of deep eutectic solvents in analytical chemistry. *Microchem J* **135**:33–38 (2017).
25. Li T, Yin Y, Wu S and Du X, Effect of deep eutectic solvents-regulated lignin structure on subsequent pyrolysis products selectivity. *Bioresour Technol* **343**:126120 (2022).
26. Ling JKU and Hadinoto K, Deep eutectic solvent as green solvent in extraction of biological macromolecules. *Int J Mol Sci* **23**:3381 (2022).
27. Zhou M, Fakayode OA, Ren M, Li H, Liang J and Zhou C, Green and sustainable extraction of lignin by deep eutectic solvent, its antioxidant activity, and applications in the food industry. *Crit Rev Food Sci Nutr* (2023). <https://doi.org/10.1080/10408398.2023.2181762>.
28. Wise EL and Karl H, *Cellulose and Hemicelluloses in Pulp and Paper Science and Technology*, Vol. 1. Pulp. McGraw Hill-Book Co, New York (1962).
29. *TAPPI T 222 Om-02, Acid-Insoluble Lignin in Wood and Pulp*. Technical Association of the Pulp and Paper Industry, Atlanta, GA (2002).
30. Lua AC, Lau FY and Guo J, Influence of pyrolysis conditions on pore development of oil-palm-shell activated carbons. *J Anal Appl Pyrolysis* **76**:96–102 (2006).
31. Cai J, He Y, Yu X, Banks SW, Yang Y, Zhang X *et al.*, Review of physicochemical properties and analytical characterization of lignocellulosic biomass. *Renew Sustain Energy Rev* **76**:309–322 (2017).
32. Klass DL, *Biomass for Renewable Energy, Fuels, and Chemicals*. Elsevier Science, San Diego (1998).
33. ASTM D7582-15, Standard Test Methods for Proximate Analysis of Coal and Coke by Macro Thermogravimetric Analysis. West Conshohocken, PA: ASTM International, (2015).
34. García R, Pizarro C, Lavín AG and Bueno JL, Biomass proximate analysis using thermogravimetry. *Bioresour Technol* **139**:1–4 (2013).
35. Cantrell K, Martin J and Ro K, Application of thermogravimetric analysis for the proximate analysis of livestock wastes. *J ASTM Int* **7**:102583 (2010).
36. Méndez P, Nuñez C, Cabrera-Pardo JR, Paz C, Barraza JM, Castillo R *et al.*, Adsorption ability of activated carbon obtained from sub-bituminous coal (Lebu, Chile) to capture trimethylamine. *J Chil Chem Soc* **64**:4582–4585 (2019).
37. Misran E, Maulina S, Dina SF, Nazar A and Harahap SA, Activated carbon production from bagasse and banana stem at various times of carbonization. *Mater Sci Eng* **309**:012064 (2018).
38. Maulina S and Iriansyah M, Characteristics of activated carbon resulted from pyrolysis of the oil palm fronds powder. *Mater Sci Eng* **309**:012072 (2018).
39. Duan XH, Srinivasakannan C, Yang KB, Peng JH and Zhang LB, Effects of heating method and activating agent on the porous structure of activated carbons from coconut shells. *Waste Biomass Valorization* **3**:131–139 (2012).
40. Hidayu AR, Mohamad NF, Matali S and Sharifah ASAK, Characterization of activated carbon prepared from oil palm empty fruit bunch using BET and FT-IR techniques. *Procedia Eng* **68**:379–384 (2013).
41. Ali R, Aslam Z, Shawabkeh RA, Asghar A and Hussein IA, BET, FTIR, and RAMAN characterizations of activated carbon from waste oil fly ash. *Turk J Chem* **44**:279–295 (2020).
42. Thommes M, Kaneko K, Neimark AV, Olivier JP, Rodriguez-Reinoso F, Rouquerol J *et al.*, Physisorption of gases, with special reference to the evaluation of the surface area and pore size distribution (IUPAC technical report). *Pure Appl Chem* **87**:1051–1069 (2015).
43. Gurten Inal II, Koyuncu F and Perez-Page M, Improving the rate capability of microporous activated carbon-based supercapacitor electrodes using non-porous graphene oxide. *J Porous Mater* **13**:1775–1787 (2023).
44. Huang K, Chai SH, Mayes RT, Tan S, Jones CW and Dai S, Significantly increasing porosity of mesoporous carbon by

- NaNH₂ activation for enhanced CO₂ adsorption. *Microporous Mesoporous Mater* **230**:100–108 (2016).
45. Ergun ME and Ergun H, Influence of activated carbon concentration on foam material properties: Design and optimization. *Arab J Sci Eng* (2023). <https://doi.org/10.1007/s13369-023-08275-w>.
 46. Rodríguez-Reinoso F, Lopez-Gonzalez JDD and Berenguer C, Activated carbons from almond shells – I: Preparation and characterization by nitrogen adsorption. *Carbon* **20**:513–518 (1982).
 47. Bülbül Ş and Ergün H, Investigation of the usability of activated carbon as a filling material in nitrile butadiene rubber/natural rubber components and modeling by regression analysis. *J Elastomers Plast* (2023). <https://doi.org/10.1177/00952443231215469>.
 48. González-García P, Activated carbon from lignocellulosic precursors: A review of the synthesis methods, characterization techniques, and applications. *Renew Sustain Energy Rev* **82**:1393–1414 (2018).
 49. Ioannidou O and Zabanitouta A, Agricultural residues as precursors for activated carbon production. *Renew Sustain Energy Rev* **11**:1966–2005 (2007).
 50. Gundogdu A, Duran C, Senturk HB, Soylak M, Imamoglu M and Onal Y, Physicochemical characteristics of a novel activated carbon produced from tea industry waste. *J Anal Appl Pyrolysis* **104**:249–259 (2013).
 51. Deng H, Yang L, Tao G and Dai J, Preparation and characterization of activated carbon from cotton stalk by microwave-assisted chemical activation – application in methylene blue adsorption from aqueous solution. *J Hazard Mater* **166**:1514–1521 (2009).
 52. Han G, Jia J, Liu Q, Huang G, Xing B, Zhang C et al., Template-activated bifunctional soluble salt ZnCl₂ assisted synthesis of coal-based hierarchical porous carbon for high-performance super capacitors. *Carbon* **186**:380–390 (2022).
 53. Alotman Z, Habila M and Ali R, Preparation of activated carbon using the co-pyrolysis of agricultural and municipal solid wastes at a low carbonization temperature. *Carbon* **24**:67–72 (2011).
 54. Nicolae SA, Szilágyi PÁ and Titirici MM, Soft templating production of porous carbon adsorbents for CO₂ and H₂S capture. *Carbon* **169**:193–204 (2020).
 55. Saka C, BET, TG-DTG, FT-IR, SEM, iodine number analysis, and preparation of activated carbon from acorn shell by chemical activation with ZnCl₂. *J Anal Appl Pyrolysis* **95**:21–24 (2012).
 56. Singh BK and Rawat NS, Comparative sorption kinetic studies of phenolic compounds on fly ash and impregnated fly ash. *J Chem Technol Biotechnol* **61**:57–65 (1994).
 57. Lawtae P and Tangsathikulchai C, The use of high surface area mesoporous-activated carbon from longan seed biomass for increasing capacity and kinetics of methylene blue adsorption from aqueous solution. *Molecules* **26**:6521 (2021).
 58. Anisuzzaman SM, Joseph CG, Krishnaiah D, Bono A, Suali E, Abang S et al., Removal of chlorinated phenol from aqueous media by guava seed (*Psidium guajava*) tailored activated carbon. *Water Resour Ind* **16**:29–36 (2016).
 59. Heidarinejad Z, Dehghani MH, Heidari M, Javedan G, Ali I and Sillanpää M, Methods for preparation and activation of activated carbon: A review. *Environ Chem Lett* **18**:393–415 (2020).
 60. Widiyastuti W, Rois MF, Setyawan H, Machmudah S and Anggoro D, Carbonization of lignin extracted from liquid waste of coconut coir delignification. *Indones J Chem* **20**:842–849 (2020).
 61. Sebbahi S, Ahmido A, Kifani-Sahban F, El Hajjaji S and Zoulalian A, Preoxidation and activation of the lignin char: Carbonization and oxidation procedures. *J Eng* **2014**:1–9 (2014).
 62. De Rose E, Bartucci S, Bonaventura CP, Conte G, Agostino RG and Policicchio A, Effects of activation temperature and time on porosity features of activated carbons derived from lemon peel and preliminary hydrogen adsorption tests. *Colloids Surf A Physicochem Eng Asp* **2023**:131727 (2023).
 63. Hayashi JI, Kazehaya A, Muroyama K and Watkinson AP, Preparation of activated carbon from lignin by chemical activation. *Carbon* **38**:1873–1878 (2000).
 64. Carrott PJM and Carrott MR, Lignin—from natural adsorbent to activated carbon: A review. *Bioresour Technol* **98**:2301–2312 (2007).
 65. Freitas JV, Nogueira FG and Farinas CS, Coconut shell-activated carbon as an alternative adsorbent of inhibitors from lignocellulosic biomass pretreatment. *Ind Crops Prod* **137**:16–23 (2019).
 66. Zhou B, Liu W, Gong Y, Dong L and Deng Y, High-performance pseudocapacitors from Kraft lignin-modified active carbon. *Electrochim Acta* **320**:134640 (2019).
 67. Demirbas A, Adsorption of lead and cadmium ions in aqueous solutions onto modified lignin from alkali glycerol delignification. *J Hazard Mater* **109**:221–226 (2004).
 68. Allen SJ, Koumanova B, Kircheva Z and Nenkova S, Adsorption of 2-nitrophenol by technical hydrolysis lignin: Kinetics, mass transfer, and equilibrium studies. *Ind Eng Chem Res* **44**:2281–2287 (2005).
 69. Martínez-Casillas DC, Mascorro-Gutiérrez I, Arreola-Ramos CE, Villafán-Vidales HI, Arancibia-Bulnes CA, Ramos-Sánchez VH et al., A sustainable approach to produce activated carbons from pecan nutshell waste for environmentally friendly super capacitors. *Carbon* **148**:403–412 (2019).
 70. Liu S, Wei W, Wu S and Zhang F, Preparation of hierarchical porous activated carbons from different industrial lignin for highly efficient adsorption performance. *J Porous Mater* **27**:1523–1533 (2020).
 71. Dittmann D, Eisentraut P, Goedecke C, Wiesner Y, Jekel M, Ruhl AS et al., Specific adsorption sites and conditions derived by thermal decomposition of activated carbons and adsorbed carbamazepine. *Sci Rep* **10**:6695 (2020).
 72. Kaya M, Şahin Ö and Saka C, Preparation and TG/DTG, FT-IR, SEM, BET surface area, iodine number and methylene blue number analysis of activated carbon from pistachio shells by chemical activation. *Int J Chem React Eng* **16**:20170060 (2017).



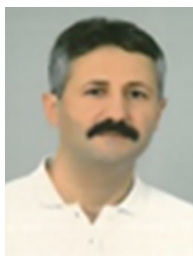
Deniz Aydemir

Deniz Aydemir is a Professor in the Department of Forest Industry Engineering at Bartın University. His studies focus on polymeric composites, biomaterials and bioplastics, value added materials from wood and recycled plastics, and

wood science and technology.

**Mehmet Emin Ergun**

Mehmet Emin Ergun is an Assistant Professor at Forestry and Forest Products, Akseki Vocational Schools, Alanya Alaaddin Keykubat University. His research topics focus on biomass conversion, renewable materials and green chemistry.

**Sezgin Koray Gulsoy**

Sezgin Koray Gulsoy is an Associate Professor in the Department of Forest Industry Engineering at Bartin University. His studies focus on the development of value-added products derived from deep eutectic solvent processing of various biomasses. He has experience in the pulp and paper industry.

**Zeynep Eda Ozan**

Zeynep Eda Ozan completed her undergraduate and graduate degrees in Forest Industrial Engineering at Bartin University and continues her doctorate. She completed her undergraduate degree in Business Administration at Anadolu University.

Her main research interests are biotechnology, wood anatomy, wood's electrical, mechanical properties and green materials.

**Gokhan Gunduz**

Gokhan Gunduz is a Professor in the Department of Industry Engineering at Iskenderun Technical University. His work focuses on project planning, product development, leadership, management consulting, green materials, emerging materials, wood

physics and mechanics, wood-based composites, forest products chemistry, and polymer composites.